e-ISSN 2320 –7876 www.ijfans.org
Vol.11, Iss.9, Dec 2022

Research Paper

Sol-gel combustion synthesis and characterization studies of manganese substituted nickel ferrite nanoparticles

E. Shakela [1,*], K. Rajendran [1]
[1] Department of Chemistry,
Bharath Institute of Higher Education and Research (BIHER),
Chennai-600073, Tamilnadu, India
***Corresponding authors:** eshakela1@gmail.com (E. Shakela)

Address for Correspondence

E. Shakela [1,*], K. Rajendran [1]
[1] Department of Chemistry,
Bharath Institute of Higher Education and Research (BIHER),
Chennai-600073, Tamilnadu, India
***Corresponding authors:** eshakela1@gmail.com (E. Shakela)

Abstract

Spinel ferrite nanoparticles presents fascinating application on biomedical, which aimed us to focus the recent investigations on synthesis of pure and manganese substituted nickel ferrite ($Ni_{1-x}Mn_xFe_2O_4$; x = 0.0, 0.5) nanoparticles using sol-gel combustion technique. The structure and the average crystallite size of the synthesized nanoparticles were analyzed from Powder X-Ray Diffraction studies. The vibrational bands corresponding to metal-oxygen linkage detected between 300-700 cm^{-1} were noticed from FT-IR spectral analysis. TEM analysis was used to study the morphology of the synthesized nanoparticles.

Keywords: Spinel ferrite; nanomaterials; Sol-gel combustion technique; TEM analysis.

1. Introduction

Spinel ferrite nanoparticles act as promising catalysts in waste water remediation owing to their stability and narrow band energy. Tuning of these band energy values is achieved by doping different cations at A or B sites making them appropriate for photocatalytic applications. Nickel ferrite displayed higher catalytic efficiency in degrading rhodamine and methylene blue dye than the bulk materials [1-5]. Microwave assisted synthesis of $GdFeO_3$, $EuFeO_3$, $SmFeO_3$ and $LaFeO_3$ perovskite nanomaterials showed varied degradation activity in visible light when methylene blue dye was used as an organic pollutant. Doping, coupling and composite formation are used to alter the properties resulting in surface modifications and structural morphology which thereby influences the band

energy. This narrowing in band energy values is responsible for better photocatalytic activity in the visible region [6-10]. Doping with transition metal ion in $RFeO_3$ lattice (R denoting rare-earth metal cations) modifies the optical properties of the nanomaterials enabling its enormous usage as effective photocatalysts [11-15].

These perovskite nanocatalysts were synthesized through bottom-up approach, which promises to be better synthetic methodology to obtain modules in nano range with homogeneous chemical composition, uniform size distribution, negligible defects and impurities. Various techniques for the synthesis of perovskite nanomaterials utilizing A(III) and B (II) salts as precursors are as reported in literature [16-20]. For the present study, sol-gel method was much preferred due to the better mixing of precursors and good chemical homogeneity in the product. Regeneration and reusability of these heterogeneous perovskite nano photocatalysts should not be wasted but instead it should be reused through profitable and energy conservation methods. The efficiency during regeneration process is lowered as a result of hindering of active adsorption sites by organic dyes or by the partial elimination of dynamic binding groups from the nano catalysts surface [21-25]. Hence there is scope for the synthesis of heterogenous perovskite nano photocatalysts which finds application in waste water remediation. In the present research, magnetically separable manganese doped cerium iron oxide perovskite nanocatalysts $Ni_{1-x}Mn_xFe_2O_4$ (x = 0.0, 0.5) nanoparticles synthesized via sol-gel method was investigated for the complete mineralization through photocatalytic studies using methylene blue dye as organic effluent.

2. Experimental method

2.1 Synthesis of $Ni_{1-x}Mn_xFe_2O_4$ (x = 0.0, 0.5) nanoparticles

The analytical graded chemicals were procured and used as such without any further purification**.** $Ni_{1-x}Mn_xFe_2O_4$ (x = 0.0, 0.5) nanoparticles was prepared via sol-gel route. The precursors namely citric acid and ethylene glycol was stirred in a magnetic stirrer around 100°C for about 15 minutes. The nitrates of the metals such as cerium, iron and manganese were dissolved in deionized water and kept in magnetic stirrer at 150°C. The transparent solution underwent gelation at 300°C for three hours in hot air oven and the obtained solid was sintered in muffle furnace at 800°C for eight hours. The prepared mixed metal oxides were characterized and investigated for photocatalytic application.

e-ISSN 2320 –7876 www.ijfans.org
Research Paper
Vol.11, Iss.9, Dec 2022

2.2 Photocatalytic activity

Multi-lamp photoreactor with oxygen purging was used to carry out the photocatalytic experiments. The photoreactor was fitted with 8W mercury vapor lamps emitting maximum spectral intensity at 385 nm. Initially, the study was done in a multi visible lamp photoreactor and an output power of 1.5W. The photocatalytic studies were achieved using methylene blue dye as an organic effluent with known concentration of 25 ppm for all the synthesized nano photocatalysts. The reaction was performed both in the presence and absence of light. After the completion of dark reaction, the process was continued by exposing the solution to visible lamp and the catalysts were drawn for every 30 minutes, centrifuged and studied for its decolourization, and mineralization efficiency.

3. Results and Discussion

3.1 Structural Analysis

The powder X-ray diffraction patterns of the synthesized materials were as shown in Fig.1. The average crystallite size determined using Scherrer equation was found to be 30-35 nm for $Ni_{1-x}Mn_xFe_2O_4$ (x = 0.0, 0.5) nanoparticles. Pseudo cubic structure with orthorhombic symmetry was exhibited by the synthesized materials. No additional secondary phases were detected in the patterns [26-28]. The initiation of ferrite formation was due to the diffraction peak at 33°.16" associated with (311) plane [29, 30]. The mixed metal oxide $Ni_{1-x}Mn_xFe_2O_4$ nanoparticles as noticed in Fig.1.

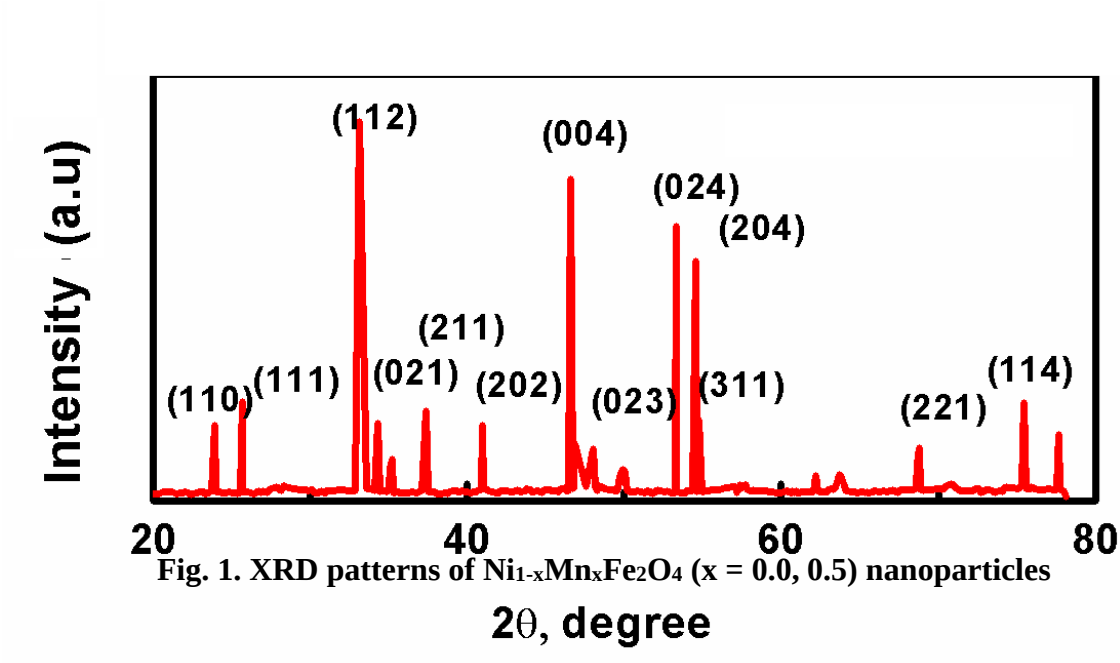

Fig. 1. XRD patterns of $Ni_{1-x}Mn_xFe_2O_4$ (x = 0.0, 0.5) nanoparticles

e-ISSN 2320 –7876 www.ijfans.org
Vol.11, Iss.9, Dec 2022

Research Paper

3.2 FT-IR Analysis

The FT-IR spectra of $CeMn_xFe_{1-x}O_{3-\delta}$ (x= 0, 0.5 and 1) nanoparticles are as presented in Fig. 2, confirmed the presence of metal-oxygen linkage within the frequency limit of 1000 cm^{-1}. Mn-O vibrations at 685 cm^{-1} and 655 cm^{-1} was detected in MnO_6 octahedron and the bending vibration of O-Fe-O bond was observed at 488 cm^{-1} in cerium ferrite structure. The peaks at 3450 cm^{-1} and 1630 cm^{-1} might be due to O-H stretching vibrations, H-O-H bending vibrations of moisture during KBr compaction and organic moieties from citric acid. On doping, a shift to reduced values, (3424 cm^{-1} and 1618 cm^{-1}) was noticed due to the lesser atomic weight of manganese compared to iron [31-35].

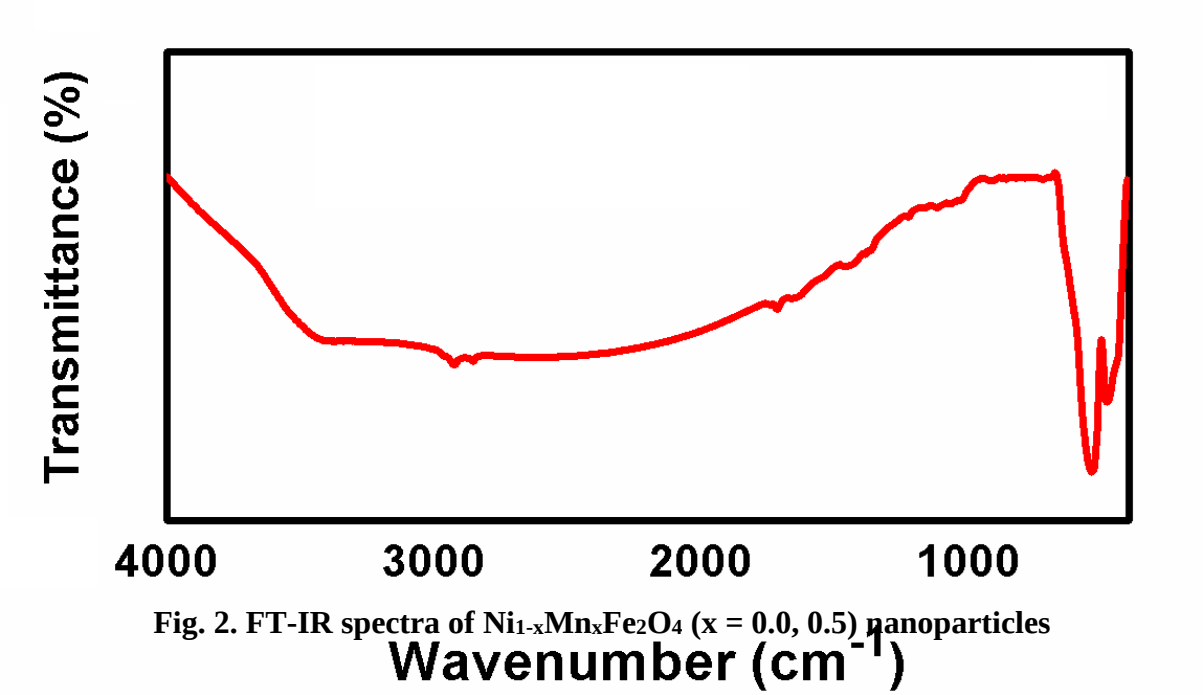

Fig. 2. FT-IR spectra of $Ni_{1-x}Mn_xFe_2O_4$ (x = 0.0, 0.5) nanoparticles

3.3 TEM Analysis

The morphology of the prepared nano mixed metal oxides sintered at 800°C was analysed from TEM studies (Fig.3). Irregular bead-shaped morphology was observed for all the prepared materials. The diameters of the rings were associated to the interplanar distances found in manganese doped cerium iron oxide structure were from the Selected Area Diffraction (SAED) patterns. The spacings obtained from the SAED patterns were reliable with the crystal planes of the orthorhombic structure as obtained in PXRD results. The

predominant degree of agglomeration of nanomaterials was due to the presence of iron in the synthesized nanomaterials [36].

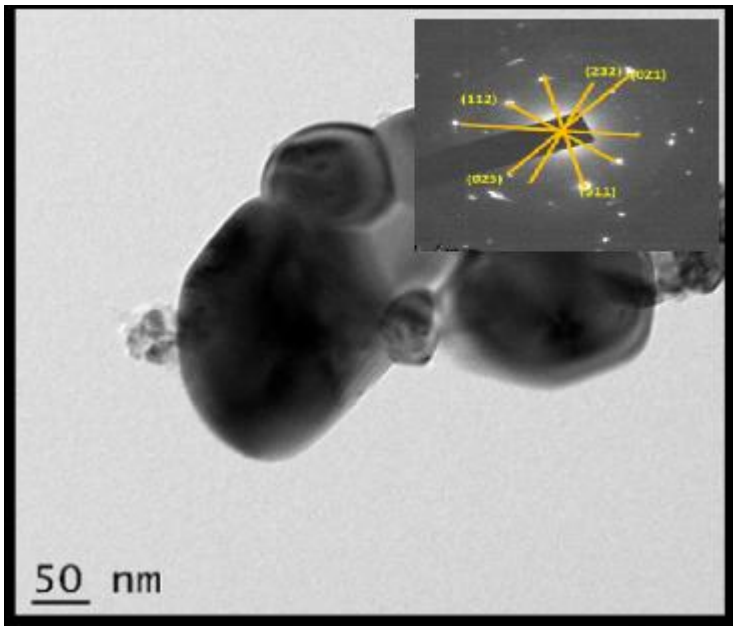

Fig. 3. TEM and SAED patterns of $Ni_{1-x}Mn_xFe_2O_4$ (x = 0.5) nanoparticles

3.4 VSM Analysis

The hysteresis loops of the prepared mixed metal oxides at room temperature are as shown in Fig. 4. Tilted spin of iron and disordered surface spins [37] are the reason for the ferromagnetic behaviour of the materials. A weak ferromagnetic behaviour was perceived for all the prepared oxide materials. Higher coercivity value and zero magnetic moment due to spin canted antiferromagnetic behavior was noticed for cerium ferrite. However, the decreased coercivity and increased magnetization values on doping manganese makes the material to act as soft magnets. The presence of oxygen vacancies disturbed antiparallel spin ordering in Fe^{3+}-O-Fe^{3+} by super exchange interactions [38].

e-ISSN 2320 –7876 www.ijfans.org
Vol.11, Iss.9, Dec 2022

Research Paper

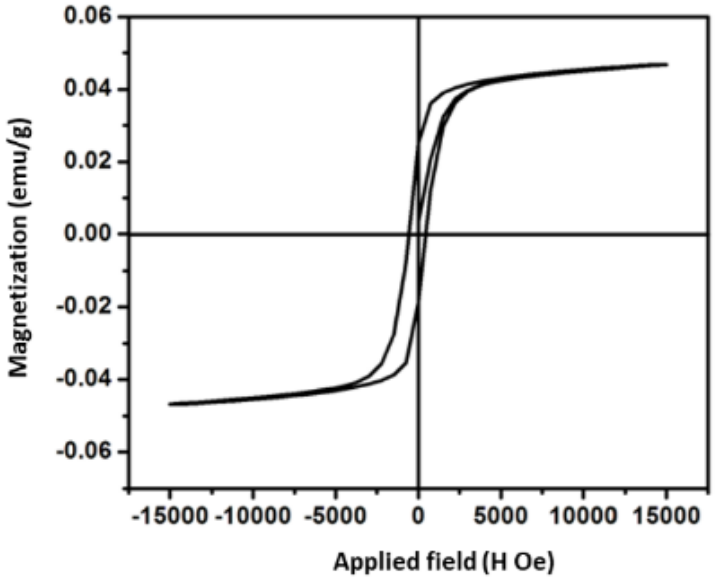

Fig. 4. VSM results of $Ni_{1-x}Mn_xFe_2O_4$ (x = 0.5) nanoparticles

3.5 Optical Analysis

UV-Visible spectroscopic studies (Fig.5) were used to study the optical properties of the prepared mixed oxide nanomaterials. The band gap values attained from the plot between $[F(R)h\nu]^2$ and photon energy (Fig.6) was estimated to be 2.38 eV for $Ni_{1-x}Mn_xFe_2O_4$ (x = 0.5) nanoparticles, however, on doping manganese, the band gap value decreased to 2 eV spinel $Ni_{1-x}Mn_xFe_2O_4$ (x = 0.0), owing to the introduction of defects related to the dopant that created confined states in the band-gap region [39-41].

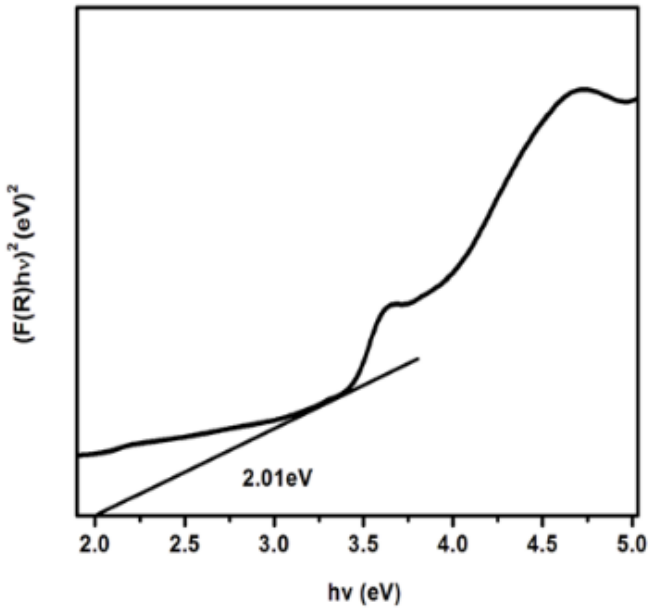

Fig. 5. Band gap values of $Ni_{1-x}Mn_xFe_2O_4$ (x = 0.5) nanoparticles

e-ISSN 2320 –7876 www.ijfans.org
Vol.11, Iss.9, Dec 2022

Research Paper

3.6 Photocatalytic application

The time-dependent photo-decolorization plots are as exemplified in Fig.7. The natural decay rate of MB dye was found to be merely about 1.80% after 180 minutes of illumination under visible lamp in the absenteeism of catalysts. Spinel $Ni_{1-x}Mn_xFe_2O_4$ (x = 0.5) nanoparticles revealed excellent photocatalytic response as a result of their extensive utilization of visible light. In the dark reaction, the rate of decolorization of the dye was found to be very low when in contact with the photocatalytic surface. This revealed that doping with transition metal ion like manganese and iron has a progressive effect, thereby enabling the metal to transfer excited electrons and decline the recombination of charge carriers.

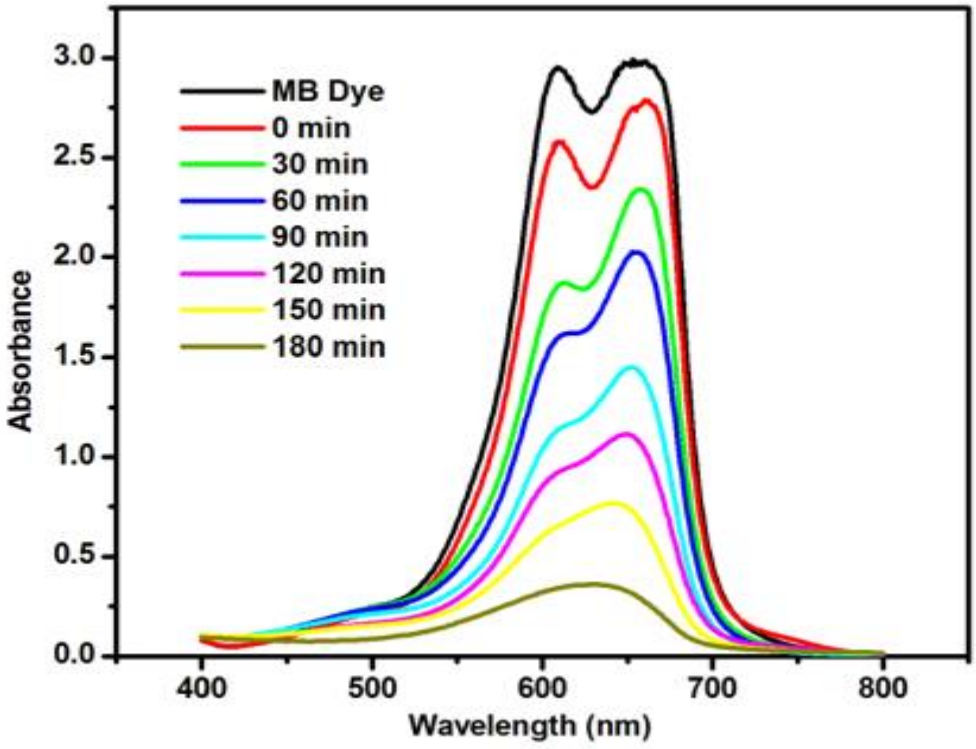

Fig. 6. Photocatalytic activity of $Ni_{1-x}Mn_xFe_2O_4$ (x = 0.5) nanoparticles

4. Conclusions

Spinel $Ni_{1-x}Mn_xFe_2O_4$ (x = 0.0, 0.5) nanoparticles was synthesized via sol-gel route. The structural analysis revealed orthorhombic symmetry with the average crystallite size of about 30 nm. The metal-oxygen linkages from the FT-IR analysis were obtained between 1000-400 cm^{-1} for all the prepared nanomaterials. The magnetic analysis indicated the weak ferromagnetic nature, increased magnetization and decreased coercivity values for the doped materials. Band gap energies evaluated from optical analysis showed decreased values on

doping manganese. Photocatalytic activity and the mineralization efficiency were higher in manganese doped mixed metal oxide material, presenting $Ni_{1-x}Mn_xFe_2O_4$ (x = 0.5) material as a better photocatalyst for dye degradation in waste-water treatment.

References

1. M. A. Almessiere, S. Güner, Y. Slimani, A. Baykal, S. E. Shirsath, A. D. Korkmaz, R. Badar, A. Manikandan, Investigation on the structural, optical, and magnetic features of Dy^{3+} and Y^{3+} co-doped $Mn_{0.5}Zn_{0.5}Fe_2O_4$ spinel ferrite nanoparticles, Journal of Molecular Structure 1248, 131412 (2022).
2. H. Tombuloglu, N. Albenayyan, Y. Slimani, S. Akhtar, G. Tombuloglu, M. Almessiere, A. Baykal, I. Ercan, H. Sabit, A. Manikandan, Fate and impact of maghemite (γ-Fe_2O_3) and magnetite (Fe_3O_4) nanoparticles in barley (Hordeum vulgare L.), Environmental Science and Pollution Research, 29 (3), 4710-4721.
3. A. Alagarsamy, S. Chandrasekaran, A. Manikandan, Green synthesis and characterization studies of biogenic zirconium oxide (ZrO_2) nanoparticles for adsorptive removal of methylene blue dye, Journal of Molecular Structure, 1247 (2022) 131275.
4. M. P. Mani, A. A. M. Faudzi, S. Mohamaddan, A. F. Ismail, R. Rathanasamy, A. Manikandan, S. K.Jaganathan, Engineered polymer matrix novel biocompatible materials decorated with eucalyptus oil and zinc nitrate with superior mechanical and bone forming abilities, Arabian Journal of Chemistry, 15, 2022, 104079.
5. M. A. Almessiere, Y. Slimani, S. Ali, A. Baykal, R. J. Balasamy, S. Guner, İ. A Auwal, A. V Trukhanov, S. V. Trukhanov, A. Manikandan, Impact of Ga^{3+} Ions on the Structure, Magnetic, and Optical Features of Co-Ni Nanostructured Spinel Ferrite Microspheres, Nanomaterials, 2022, 12(16), 2872.
6. A. Khan, A. A. P. Khan, H. M. Marwani, M. M. Alotaibi, A. M. Asiri, A. Manikandan, S. Siengchin, S. M. Rangappa, Sensitive Non-Enzymatic Glucose Electrochemical Sensor Based on Electrochemically Synthesized PANI/Bimetallic Oxide Composite, Polymers, 2022, 14(15), 3047.
7. A. P. Subramanian, S. K. Jaganathan, A. Manikandan, K. N. Pandiaraj, N. Gomathi and E. Supriyanto, Recent trends in nano based drug delivery systems for efficient delivery of phytochemicals in chemotherapy, RSC Advances, 6 (2016) 48294-48314.

8. M. A. Almessiere, Y. Slimani, H. Güngüneş, S. Ali, A. Manikandan, I. Ercan, A. Baykal, A.V. Trukhanov, Magnetic Attributes of $NiFe_2O_4$ Nanoparticles: Influence of Dysprosium Ions (Dy^{3+}) Substitution, Nanomaterials, 9 (2019) 820.
9. V. Muthuvignesh, V.J. Reddy, S. Ramakrishna, S. Ray, A. Ismail, M. Mandal, A. Manikandan, S. Seal and S. K. Jaganathan, Electrospinning applications from diagnosis to treatment of diabetes, RSC Advances, 6 (2016) 83638-83655.
10. V. Muthuvignesh, S. K. Jaganathan, A. Manikandan, Nanomaterials as a game changer in the management and treatment of diabetic foot ulcers, RSC Advances, 6 (2016) 114859-114878.
11. A. Manikandan, A. Saravanan, S. Arul Antony, M. Bououdina, One-pot low temperature synthesis and characterization studies of nanocrystalline α-Fe_2O_3 based dye sensitized solar cells, Journal of Nanoscience and Nanotechnology, 15 (2015) 4358-4366.
12. S. Asiri, S. Güner, A. Demir, A. Yildiz, A. Manikandan, A. Baykal, Synthesis and Magnetic Characterization of Cu Substituted Barium Hexaferrites, Journal of Inorganic and Organometallic Polymers and Materials, 28 (2018) 1065–1071.
13. D. K. Manimegalai, A. Manikandan, S. Moortheswaran, S. Arul Antony, Magneto-Optical and Photocatalytic Properties of Magnetically Recyclable $Zn_{1-x}Mn_xS$ (x = 0.0, 0.3 and 0.5) nano-catalysts, Journal of Superconductivity and Novel Magnetism, 28 (2015) 2755-2766.
14. P. Thilagavathi, A. Manikandan, S. Sujatha, S. K. Jaganathan, S. Arul Antony, Sol-gel synthesis and characterization studies of $NiMoO_4$ nanostructures for photocatalytic degradation of methylene blue dye, Nanoscience and Nanotechnology Letters, 8 (2016) 438-443.
15. G. Mathubala, A. Manikandan, S. Arul Antony, P. Ramar, Enhanced photocatalytic activity of spinel $Cu_xMn_{1-x}Fe_2O_4$ nanocatalysts for the degradation of methylene blue dye and opto-magnetic properties, Nanoscience and Nanotechnology Letters, 8 (2016) 375-381.
16. D. Vanitha, B. Sultan Asath, N. Nallaperumal, A. Shunmuganarayanan, A. Manikandan, Electrical Impedance studies on sodium ion conducting composite blend polymer electrolyte, Journal of Inorganic and Organometallic Polymers and Materials, 27 (2017) 257–265.

17. K. Geetha, R. Udhayakumar, A. Manikandan, Enhanced magnetic and photocatalytic characteristics of cerium substituted spinel $MgFe_2O_4$ ferrite nanoparticles, Physica B: Physics of Condensed Matter, 615 (2021) 413083, Impact Factor: 2.436. (Elsevier)
18. S. S. Al-Jameel, S. Rehman, M. A. Almessiere, F. A. Khan, Y. Slimani, N. S. Al-Saleh, A. Manikandan, E. A. Al-Suhaimi, A. Baykal, Anti-microbial and anti-cancer activities of $MnZnDy_xFe_{2-x}O_4$ ($x \leq 0.1$) nanoparticles, Artificial Cells, Nanomedicine and Biotechnology, 49 (2021) 493-499.
19. S. Rehman, M. A. Almessiere, S. S. Al-Jameel, U. Ali, Y. Slimani, N. Taskhandi, N. S. Al-Saleh, A. Manikandan, F. A. Khan, E. A. Al-Suhaimi, A. Baykal, Designing of $Co_{0.5}Ni_{0.5}Ga_xFe_{2-x}O_4$ ($0.0 \leq x \leq 1.0$) Microspheres via Hydrothermal Approach and Their Selective Inhibition on the Growth of Cancerous and Fungal Cells, Pharmaceutics, 13 (2021) 962.
20. C. Sambathkumar, R. Ranjithkumar, S. Ezhil Arasi, A. Manikandan, N. Nallamuthu, M. Krishna Kumar, A. Arivarasan, P. Devendran, High-performance nickel sulfide modified electrode material from single source precursor for energy storage application, Journal of Materials Science: Materials in Electronics, 32 (2021) 20058-20070.
21. C. Sambathkumar, V. Manirathinam, A. Manikandan, M. Krishna Kumar, S. Sudhakar, P. Devendran, Solvothermal synthesis of Bi_2S_3 nanoparticles for active photocatalytic and energy storage device applications, Journal of Materials Science: Materials in Electronics, 32 (2021) 20827-20843.
22. V. S. P. Sakthi Sri, A. Manikandan, M. Mathankumar, R. Tamizhselvi, M. George, A. L. Bilgrami, S. A. Al-Zahrani, A. A. P. Khan, Anish Khan, A. M. Asiri, Unveiling the photosensitive, mechanical and magnetic properties of amorphous iron nanoparticles with its application towards decontamination of water and cancer treatment, Journal of Materials Research and Technology, 15 (2021) 99-118.
23. M. A. Almessiere, B. Unal, Y. Slimani, H. Gungunes, M. S. Toprak, N. Tashkand, A. Baykal, M. Sertkol, A.V. Trukhanov, A. Yıldız, A. Manikandan, Effects of Ce-Dy rare earths co-doping on various features of Ni-Co spinel ferrite microspheres prepared via hydrothermal approach, Journal of Materials Research and Technology, 14 (2021) 2534-2553.
24. S. Blessi, A. Manikandan, S. Anand, M. M. L. Sonia, V. M. Vinosel, P. Paulraj, Y. Slimani, M.A. Almessiere, M. Iqbal, S. Guner, A. Baykal, Effect of Zinc substitution

on the physical and electrochemical properties of mesoporous SnO_2 nanomaterials, Materials Chemistry and Physics, 273 (2021) 125122.

25. M. A. Almessiere, Y. Slimani, Y. O. Ibrahim, M. A. Gondal, M. A. Dastageer, I. A. Auwal, A. V. Trukhanov, A. Manikandan, A. Baykal, Morphological, structural, and magnetic characterizations of hard-soft ferrite nanocomposites synthesized via pulsed laser ablation in liquid, Materials Science and Engineering B, 273 (2021) 115446.
26. M. A. Almessiere, Y. Slimani, N. A. Algarou, M. A. Gondal, Y. S. Wudil, M. Younas, I. A. Auwal, A. Baykal, A. Manikandan, T. I. Zubar, V. G. Kostishin, A. V. Trukhanov, I. Ercan, Electronic, magnetic, and microwave properties of hard/soft nanocomposites based on hexaferrite $SrNi_{0.02}Zr_{0.02}Fe_{11.96}O_{19}$ with variable spinel phase MFe_2O_4 (M = Mn, Co, Cu, and Zn), Ceramics International, 47 (2021) 35209-35223.
27. M. A. Almessiere, Y. Slimani, N. A. Algarou, M. A. Gondal, Y. S. Wudil, M. Younas, I. A. Auwal, A. Baykal, A. Manikandan, Electrospinning synthesis of Cd substituted Ni-Co spinel ferrite nanofibers: An investigation on their structural and magnetic features, Applied Physics A, 127 (2021) 785.
28. M. A. Almessiere, Y. Slimani, N. A. Algarou, M. A. Gondal, Y. S. Wudil, M. Younas, I. A. Auwal, A. Baykal, A. Manikandan, Investigation on electrical and dielectric properties of hard/soft spinel ferrite nanocomposites of $CoFe_2O_4/(NiSc_{0.03}Fe_{1.97}O_4)x$, Vacuum, 194 (2021) 110628,
29. N. Kabeerdass, A. Al Otaibi, M. Rajendran, A. Manikandan, H. A. Kashmery, M. M. Rahman, P. Madhu, A. Khan, A. M. Asiri, M. Mathanmohun, Bacillus-Mediated Silver Nanoparticle Synthesis and Its Antagonistic Activity against Bacterial and Fungal Pathogens, Antibiotics, 10 (2021) 1334.
30. C. R. T. Kumari, A. Al Otaibi, T. Kamaraj, M. Nageshwari, G. Mathubala, A. Manikandan, M. L. Caroline, S. Sudha, H. A. Kashmery, P. Madhu, A. Khan, H. M. Marwani, A. M. Asiri, A brief study on optical and mechanical properties of an organic material: urea glutaric acid (2/1)-a third order nonlinear optical single crystal, Crystals, 11 (2021) 1239.
31. R. R. Mathiarasu, A. Manikandan, K. Panneerselvam, M. George, Y. Slimani, M. A. Almessiere, A. Baykal, A. M. Asiri, T. Kamal, A. Khan, Photocatalytic degradation of reactive anionic dyes RB5, RR198 and RY145 via Rare earth element (REE)

Lanthanum substituted $CaTiO_3$ perovskite catalysts, Journal of Materials Research and Technology, 15 (2021) 5936-5947.

32. M.A. Almessiere, N.A. Algarou, Y. Slimani, A. Sadaqat, A. Baykal, A. Manikandan, S.V. Trukhanov, A.V. Trukhanov, I. Ercan, Investigation of exchange coupling and microwave properties of hard/soft $(SrNi_{0.02}Zr_{0.01}Fe_{11.96}O_{19})/(CoFe_2O_4)x$ nanocomposites, Materials Today Nano, 18 (2022) 100186.
33. M. P. Mani, A.A.M. Faudzi, S. Mohamaddan, A. F. Ismail, R. Rajasekar, A. Manikandan, S. K. Jaganathan, Grapefruit oil and cobalt nitrate loaded polyurethane hybrid nanofibrous scaffold for biomedical applications, Frontiers in Materials Biomaterials, 9 (2022) 827009.
34. S. A. Al-Zahrani, A. Manikandan, K. Thanrasu , A. Dinesh, K. K. Raja, M.A. Almessiere, Y. Slimani, A. Baykal, S. Bhuminathan, S. R. Jayesh, J. Ahmed, H. S. Alorfi, M. A. Hussein, I. Khan, A. Khan, Influence of Ce^{3+} on the structural, morphological, magnetic, photocatalytic and antibacterial properties of spinel $MnFe_2O_4$ nanocrystals prepared by combustion route, Crystals, 12 (2022) 268.
35. B. Unal, M. A. Almessiere, A. V. Trukhanov, A. Baykal, Y. Slimani, M. V. Silibin, A. Ul-Hamid, A. Manikandan, A study on the conductivity, dielectric, and microwave properties of $(SrNb_xY_xFe_{12-2x}O_{19}$ $(0.00 \leq x \leq 0.05)$ nanohexaferrites, Journal of Materials Research and Technology, 17 (2022) 2975-2986.
36. B. A. Kumar, V. Vetrivelan, G. Ramalingam, A. Manikandan, S. Viswanathan, P. Boomi, G. Ravi, Computational studies and experimental fabrication of DSSC device assembly on 2D-layered TiO_2 and $MoS_2@TiO_2$ nanomaterials, Physica B: Condensed Matter, 633 (2022) 413770.
37. T.L. Ajeesha, A. Manikandan, A. Ashwini, Sagaya Jansi, M. Durka, M. A. Almessiere, Y. Slimani, A. Baykal, A. M. Asiri, H. A. Kasmery, A. Khan, A.A.P. Khan, P. Madhu, M. George, Structural investigation of Cu doped calcium ferrite $(Ca_{1-x}Cu_xFe_2O_4$; x = 0, 0.2, 0.4, 0.6, 0.8, 1) nanomaterials prepared by co-precipitation method, Journal of Materials Research and Technology, 18 (2022) 705-719.
38. M. Sertkol, S. Güner, M. A. Almessiere, Y. Slimani, A. Baykal, H. Gungunes, E. M. Alsulami, F. Alahmari, M. A. Gondal, S. E. Shirsath, A. Manikandan, Effect of Bi^{3+} ions substitution on the structure, morphology, and magnetic properties of Co-Ni spinel ferrite nanofibers, Materials Chemistry and Physics, 284 (2022) 126071.

39. A. Dinesh, K. Kanmani Raja, A. Manikandan, M. A. Almessiere, Y. Slimani, A. Baykal, H. S. Alorfi, M. A. Hussein, A. Khan, Sol-gel combustion synthesis and photocatalytic dye degradation studies of rare earth element Ce substituted Mn-Zn ferrite nanoparticles, Journal of Materials Research and Technology, 18 (2022) 5280-5289,
40. Y. Slimani, M. A. Almessiere, A. D. Korkmaz, A. Baykal, A. Manikandan, H. Gungunes, M. S. Toprak, Ultrasound-assisted synthesis and magnetic investigations of $Ni_{0.4}Cu_{0.4}Zn_{0.2}Ga_xGd_xFe_{2-2x}O_4$ ($0.00 \leq x \leq 0.04$) nanosized spinel ferrites, Applied Physics A 128 (2022) 1-14.
41. M. Sertkol, Y. Slimani, M.A. Almessiere, H. Sozeri, R. Jermy, A. Manikandan, S.E. Shirsath, A. UI-Hamid, A. Baykal, Sonochemical synthesis of $Mn_{0.5}Zn_{0.5}Er_xDy_xFe_{2-2x}O_4$ ($x \leq 0.1$) spinel nanoferrites: Magnetic and textural investigation, Journal of Molecular Structure, 1258 (2022) 132680.